

Supplemental Information

Methods and Materials

Paradigm: Explicit emotion labeling tasks

All stimuli were gray-scale digitized photographs from the Pictures of Facial Affect, morphed using software to depict emotional expressions ranging from neutral (0%) to mild (50%) to intense (100%) emotion in each experiment (1). Each stimulus was $15 \times 10.5 \text{ cm}^2$, presented centrally and masked (hair and non-face features removed) for 2s, with a mean inter-stimulus interval of 4.9s during which a fixation cross was displayed.

Data acquisition

MRI scans were acquired with a 3T Siemens Magnetom Allegra syngo MR-2004A at the Brain Imaging Research Center, University of Pittsburgh and Carnegie Mellon University, Pittsburgh, USA. A standard head coil was used for radio frequency (RF) transmission and reception of the MR signal and restraining foam pads were utilized for minimizing head motion.

Anatomical images covering the entire brain were acquired using a sagittal 3D MPRAGE sequence, parallel to the AC–PC line (TE/TR=2.48ms/1630ms, flip angle=8, field-of-view (FOV)= $200 \times 200 \text{ mm}^2$, 224 sagittal 0.8mm-thick slices, matrix size=50×250 voxels; acquisition:6':07").

Mean blood-oxygenation-level-dependent (BOLD) images were acquired using an axial gradient-echo EPI sequence, parallel to the AC–PC line (TR/TE=2000/25msec, flip angle=90, FOV= $200 \times 200 \text{ mm}^2$, thirty-three 3mm-thick slices, no gaps; matrix=64x64, EPI factor=64; acquisition:6':06").

Diffusion tensor data were acquired using a coronal diffusion-weighted single-shot spin-echo planar imaging sequence, parallel to the AC–PC line (TR=4400ms, TE=76ms, bandwidth 1860[Hz/Px], flip angle=90, FOV=200×200 mm², thirty-three 3mm-thick slices, no-gaps, matrix size=80x128, EPI factor=128; acquisition:6':16"). Two b values were used: one $b=0$ (no-diffusion weighting) image and six non-coplanar $b=850\text{s/mm}^2$ (diffusion-weighting b -value) images were acquired, parameters similar to those employed in recent DTI studies (2-3). Fat saturation was used to remove scalp signal (that can disrupt neural signal owing to chemical shift or ghosting artifacts). DTI data were used in analyses of WM structure-FC relationships in the present study.

An expert radiologist screened all the MPRAGE scans for visible white matter and other pathology as part of our Institutional Review Board–approved protocol.

Data analyses

fMRI data analyses. 180-timeseries fMRI volumes acquired from each participant were corrected for differences in image acquisition time between slices and realigned using a least squares approach and a rigid body (6 parameters) spatial transformation to the first image as a reference to remove movement artifacts. Data were unwrapped to remove variance due to susceptibility-by-movement interaction. Each volume was co-registered by aligning the first scan from each volume to the first scan of the first volume with regard to the subject's MPRAGE image and segmented. All fMRI data were normalized to the standard Montreal Neurological Institute (MNI) template, resampled to $3\times 3\times 3\text{ mm}^3$ voxels, and spatially smoothed with a Gaussian kernel of 6mm full-width at half-maximum (FWHM). A first-level fixed-effect model was defined by entering three emotion intensities (neutral, mild, intense) in both experiments (happy and sad) as

separate conditions in an event-related design matrix with fixation cross as baseline. Movement parameters were entered as covariates of no interest. Time series were modeled using the Canonical Hemodynamic Response Function; ‘no global scaling’ was set. Uncorrelated low-frequency noise was removed by using high-pass filter (cut-off 128sec). Relatively short inter-stimulus intervals (<8sec) and serial correlations due to aliased biorhythms and unmodelled neural activity were accounted for by using a first-order autoregressive model (4).

DTI data analyses. Thirty-one diffusion weight images (DWI) were analyzed using the Functional Magnetic Resonance Imaging of the Brain (FMRIB) Software Library (FSL). First, data were inspected for motion artifacts, then DWI were registered to the $b=0$ image, as a reference, by affine transformations to minimize distortions due to eddy currents and reduce simple head motion, using Eddy Current Correction. Images were extracted using the Brain Extraction Tool (BET) (5), part of the FSL package (6).

A diffusion tensor model was fitted at each voxel, providing a voxelwise calculation of fractional anisotropy (FA) (7). FA can be expressed in terms of the three eigenvalues: λ_1 is the principal longitudinal diffusion direction, λ_2 and λ_3 are directions perpendicular to the principal diffusion direction, and $\bar{\lambda}$ is mean diffusion:

$$FA = \frac{\sqrt{3 \left[(\lambda_1 - \bar{\lambda})^2 + (\lambda_2 - \bar{\lambda})^2 + (\lambda_3 - \bar{\lambda})^2 \right]}}{\sqrt{2(\lambda_1^2 + \lambda_2^2 + \lambda_3^2)}}$$

Whole-brain voxelwise analysis of FA data was performed by first aligning each subject’s FA-image into a higher-resolution FA standard space (MNI atlas), according to a non-linear registration algorithm, implemented in TBSS (8-9). The derived mean FA image was minimized to generate a template-skeleton embodying the center of all tracts derived from the whole group.

An $FA \geq 0.20$ threshold was set in order to exclude peripheral tracts that might lead to erroneous interpretations due to anatomic inter-subject variability and/or partial volume effects with GM. Each subject's aligned FA data were projected onto this template-skeleton. Local FA maxima were then estimated with voxelwise, between-subject statistics, using Randomise, a TBSS statistic tool: (<http://www.fmrib.ox.ac.uk/fsl/randomise/index.html>). We used a non-parametric two-sample independent t-test to compare groups, based on a permutation method, because of the non-parametric distribution of the data. Age was entered into this analysis as a confound regressor to ensure that any observed effect of group upon FA was independent of age-related changes. We then performed the following non-parametric permutation tests to test for between-group differences in FA, as previously employed (2). We used a stringent threshold (median t value, t_{50} within the group of voxels ≥ 3 ; $p \leq 0.001$, uncorrected; number of permutations=10000; smoothing factor=5). We considered a cluster as a group of contiguous voxels with $p < 0.001$ and ≥ 5 voxels. We controlled for multiple voxel-level comparisons within each cluster showing between-group differences in FA determined in the above whole-brain analyses using a small volume correction ($p \leq 0.05$) with an anatomically-defined regional mask in the relevant WM tract, that contained approximately 100 times the number of voxels than each cluster, and False Discovery Rate (FDR), an FSL statistic tool (<http://www.fmrib.ox.ac.uk/fsl/randomise/fdr.html>). We determined the most probable anatomical localization of each cluster with the FSL atlas tool (<http://www.fmrib.ox.ac.uk/fsl/fslview/atlas-descriptions.html>), using all anatomical templates (Harvard-Oxford cortical and subcortical structural atlases, Jülich histological atlas, JHU DTI-based white-matter atlases, Oxford thalamic connectivity atlas, Talairach atlas, and MNI structural atlas). The images represent findings projected onto the WM skeleton and magnified for display purposes using the "tbss_fill" script from the FSL package.

Table S1. Regions showing greater and reduced FA in BD vs HC in the Uncinate Fasciculus (UF).

FA in BDvsHC	N of Voxels	MNI Coordinates			WM Tract	Corresponding Cortical Area	Group (N)	Mean FA (SD)	t ₅₀ value (t _{max})	P value	d
		X (mm)	Y (mm)	Z (mm)							
	7	-22	25	1	Left UF	OFC/Insula	BD (31) HC (25)	0.64 (0.06) 0.58 (0.05)	FA = 3.0 (3.3)	0.001	1.00
↑	7	-33	21	-17	Left UF	OFC	BD (31) HC (25)	0.43 (0.02) 0.29 (0.09)	FA = 4.2 (4.6)	< 0.001	1.10
	5	-37	20	-13	Left UF	OFC	BD (31) HC (25)	0.379 (0.02) 0.26 (0.08)	FA = 4.5 (5.3)	< 0.001	0.97
↓	5	14	46	-14	Right UF	OFC	BD (31) HC (25)	0.51 (0.07) 0.59 (0.08)	FA = 3.3 (3.9)	< 0.001	1.10

d, Cohen's d; WM, white matter; FA, fractional anisotropy; BD, bipolar disorder, HC, healthy controls; OFC, orbitofrontal cortex
 ↑: clusters in which FA was significantly greater in BD versus HC; ↓: clusters in which FA was significantly reduced in BD versus HC
 In **bold** FA indexes for clusters with t > 3, uncorrected p value > 0.001. All of these regions survived small volume correction (p < 0.05)

Table S2. Curve Fitting between Functional and White Matter Connectivity Measures in Amygdala-OFC FC During Sad and Happy Experiments.

		AMYGDALA-OFC FUNCTIONAL CONNECTIVITY												
		SAD					HAPPY							
		<i>R Square</i>	<i>F</i>	<i>[df]</i>	<i>Sig.</i>	<i>lower CI</i>	<i>higher CI</i>	<i>R Square</i>	<i>F</i>	<i>[df]</i>	<i>Sig.</i>	<i>lower CI</i>	<i>higher CI</i>	
LEFT														
AMYGDALA-OFC WHITE MATTER CONNECTIVITY (FRACTIONAL ANISOTROPY)	LEFT MNI [-22 25 1]	Linear	0.1	1.67	[1,28]	0.207	0.17	0.56	0.0	1.11	[1,29]	0.300	0.14	0.57
		Logarithmic	0.0	0.89	[1,28]	0.354	0.17	0.56	0.0	0.34	[1,29]	0.566	0.14	0.57
		BD Quadratic	0.1	1.73	[2,27]	0.197	0.17	0.56	0.2	3.40	[2,28]	0.048	0.15	0.56
		Cubic	0.2	1.56	[3,26]	0.222	0.17	0.56	0.2	2.33	[3,27]	0.097	0.15	0.56
		Exponential	0.1	2.12	[1,28]	0.156	0.22	0.58	0.1	1.61	[1,29]	0.215	0.20	0.60
	LEFT MNI [-33 21 -17]	Linear	0.1	1.84	[1,22]	0.188	0.06	0.56	0.0	0.00	[1,22]	0.968	0.12	0.66
		Logarithmic	0.1	2.44	[1,22]	0.133	0.07	0.56	0.0	0.04	[1,22]	0.837	0.12	0.66
		HC Quadratic	0.2	2.04	[2,21]	0.155	0.06	0.56	0.1	0.78	[2,21]	0.473	0.12	0.66
		Cubic	0.2	1.81	[3,20]	0.178	0.06	0.57	0.1	1.07	[3,20]	0.385	0.11	0.66
		Exponential	0.1	1.63	[1,22]	0.216	0.15	0.58	0.0	0.09	[1,22]	0.764	0.20	0.70
	LEFT MNI [-33 21 -17]	Linear	0.0	0.12	[1,28]	0.735	0.17	0.56	0.0	0.67	[1,29]	0.421	0.14	0.57
		Logarithmic	0.0	0.05	[1,28]	0.825	0.17	0.56	0.0	0.32	[1,29]	0.576	0.14	0.57
		BD Quadratic	0.0	0.46	[2,27]	0.638	0.16	0.57	0.1	0.87	[2,28]	0.431	0.14	0.57
		Cubic	0.1	0.82	[3,26]	0.492	0.16	0.57	0.1	0.62	[3,27]	0.608	0.13	0.58
		Exponential	0.0	0.13	[1,28]	0.725	0.21	0.59	0.0	0.74	[1,29]	0.396	0.19	0.60
	LEFT MNI [-37 20 -13]	Linear	0.2	4.59	[1,22]	0.043	0.08	0.55	0.2	6.32	[1,22]	0.020	0.15	0.63
		Logarithmic	0.1	3.28	[1,22]	0.084	0.07	0.56	0.2	4.98	[1,22]	0.036	0.14	0.63
		HC Quadratic	0.3	4.37	[2,21]	0.026	0.08	0.54	0.3	3.92	[2,21]	0.036	0.15	0.63
		Cubic	0.6	8.47	[3,20]	0.001	0.12	0.50	0.3	3.20	[3,20]	0.045	0.15	0.63
		Exponential	0.1	2.90	[1,22]	0.103	0.16	0.57	0.2	5.39	[1,22]	0.030	0.21	0.67
LEFT MNI [-37 20 -13]	Linear	0.0	0.29	[1,28]	0.593	0.17	0.56	0.0	0.25	[1,29]	0.619	0.14	0.57	
	Logarithmic	0.0	0.40	[1,28]	0.531	0.17	0.56	0.0	0.31	[1,29]	0.581	0.14	0.57	
	BD Quadratic	0.1	1.20	[2,27]	0.316	0.17	0.56	0.0	0.45	[2,28]	0.642	0.13	0.58	
	Cubic	0.1	1.20	[3,26]	0.316	0.17	0.56	0.0	0.45	[3,27]	0.642	0.13	0.58	
	Exponential	0.0	0.38	[1,28]	0.542	0.21	0.59	0.0	0.33	[1,29]	0.573	0.19	0.60	
LEFT MNI [-37 20 -13]	Linear	0.1	2.78	[1,22]	0.109	0.07	0.56	0.2	4.09	[1,22]	0.055	0.14	0.64	
	Logarithmic	0.1	2.81	[1,22]	0.108	0.07	0.56	0.2	4.31	[1,22]	0.050	0.14	0.64	
	HC Quadratic	0.1	1.35	[2,21]	0.281	0.06	0.57	0.2	2.25	[2,21]	0.130	0.13	0.65	
	Cubic	0.1	1.35	[3,20]	0.281	0.06	0.57	0.2	2.25	[3,20]	0.130	0.13	0.65	
	Exponential	0.1	2.60	[1,22]	0.121	0.16	0.57	0.1	3.60	[1,22]	0.071	0.21	0.68	
RIGHT														
RIGHT	RIGHT MNI [14 46 -14]	Linear	0.0	0.02	[1,28]	0.884	0.16	0.59	0.0	0.61	[1,29]	0.439	0.14	0.58
		Logarithmic	0.0	0.01	[1,28]	0.912	0.16	0.59	0.0	0.53	[1,29]	0.473	0.14	0.58
		BD Quadratic	0.0	0.12	[2,27]	0.889	0.16	0.59	0.0	0.59	[2,28]	0.559	0.13	0.59
		Cubic	0.0	0.11	[3,26]	0.892	0.16	0.59	0.0	0.63	[3,27]	0.538	0.13	0.59
		Exponential	0.0	0.00	[1,28]	0.961	0.21	0.64	0.0	0.48	[1,29]	0.494	0.19	0.62
	RIGHT MNI [14 46 -14]	Linear	0.0	0.34	[1,22]	0.568	0.03	0.49	0.1	1.21	[1,22]	0.283	0.15	0.61
		Logarithmic	0.0	0.19	[1,22]	0.666	0.03	0.49	0.1	1.21	[1,22]	0.283	0.15	0.61
		HC Quadratic	0.1	1.02	[2,21]	0.378	0.03	0.49	0.1	0.58	[2,21]	0.570	0.14	0.62
		Cubic	0.1	0.98	[3,20]	0.392	0.03	0.49	0.1	0.58	[3,20]	0.568	0.14	0.62
		Exponential	0.0	0.00	[1,22]	0.959	0.14	0.44	0.0	0.84	[1,22]	0.369	0.21	0.65
	RIGHT MNI [14 46 -14]	Linear	0.0	0.02	[1,28]	0.884	0.16	0.59	0.0	0.61	[1,29]	0.439	0.14	0.58
		Logarithmic	0.0	0.01	[1,28]	0.912	0.16	0.59	0.0	0.53	[1,29]	0.473	0.14	0.58
		BD Quadratic	0.0	0.12	[2,27]	0.889	0.16	0.59	0.0	0.59	[2,28]	0.559	0.13	0.59
		Cubic	0.0	0.11	[3,26]	0.892	0.16	0.59	0.0	0.63	[3,27]	0.538	0.13	0.59
		Exponential	0.0	0.00	[1,28]	0.961	0.21	0.64	0.0	0.48	[1,29]	0.494	0.19	0.62

MNI, Montreal Neurological Institute coordinates; CI, 95% confidence intervals; OFC, orbitofrontal cortex; FC, functional connectivity; BD, bipolar disorder; HC, healthy controls.

* We used a corrected statistical threshold of $p < 0.05/8 \leq 0.006$ (in **bold**) to control for the eight multiple tests in each group between left amygdala-OFC FC to all faces in both experiments and the three clusters in the region of left UF (n=6 tests per group), and between amygdala-OFC FC to all faces in both experiments and the cluster in the region of right UF (n=2 tests per group). Trend range $0.006 < p \leq 0.05$ in **bold-italic**.

Table S3. Relationships between Continuous Demographic, Clinical and Emotion Labeling Task Performance Variables and Amygdala-OFC Functional Connectivity in BD and HC

		AGE at SCAN in BD			AGE at SCAN in HC			AGE at ONSET			ILLNESS DURATION			HDRS-25			TASK PERFORMANCE (HAPPY) in BD			TASK PERFORMANCE (HAPPY) in HC			TASK PERFORMANCE (SAD) in BD			TASK PERFORMANCE (SAD) in HC																		
		r	P value	lower CI	higher CI	r	P value	lower CI	higher CI	r	P value	lower CI	higher CI	r	P value	lower CI	higher CI	r	P value	lower CI	higher CI	r	P value	lower CI	higher CI	r	P value	lower CI	higher CI	r	P value	lower CI	higher CI											
HAPPY	INTENSE	LEFT	-0.05	0.775	-35.3	64.7	-0.02	0.927	-76.3	89.7	-0.22	0.240	-8.6	89.1	0.17	0.365	-68.9	16.7	0.10	0.599	-30.2	88.4	-0.19	0.336	-67.7	42.4	-0.06	0.775	-44.5	109.3	n/a	n/a	n/a	n/a	n/a	n/a	n/a	n/a	n/a	n/a				
		RIGHT	-0.32	0.077	-88.9	19.8	0.18	0.399	-79.2	146.4	-0.48	0.006	-68.0	38.1	0.22	0.225	-68.3	24.7	-0.02	0.906	-64.0	62.3	-0.21	0.288	-29.8	89.8	0.32	0.122	-139.7	69.4	n/a	n/a	n/a	n/a	n/a	n/a	n/a	n/a	n/a	n/a	n/a			
	MILD	LEFT	0.16	0.380	-77.5	26.9	-0.01	0.971	-67.7	51.1	-0.16	0.381	-85.9	16.0	0.37	0.038	-36.8	52.6	0.18	0.334	-52.3	70.4	-0.16	0.430	-39.0	76.0	-0.41	0.049	-102.4	7.7	n/a	n/a	n/a	n/a	n/a	n/a	n/a	n/a	n/a	n/a	n/a			
		RIGHT	0.01	0.951	-34.9	85.4	0.07	0.740	-84.7	140.5	-0.27	0.136	-75.8	41.6	0.35	0.050	-1.1	101.8	0.19	0.326	-99.6	40.6	-0.08	0.698	-102.4	29.9	0.00	0.992	-30.0	178.6	n/a	n/a	n/a	n/a	n/a	n/a	n/a	n/a	n/a	n/a	n/a			
	NEUTRAL	LEFT	-0.05	0.797	-59.4	37.3	-0.02	0.938	-98.4	48.8	-0.14	0.463	-68.1	26.2	0.10	0.591	-27.9	54.7	0.25	0.181	-103.2	9.1	-0.21	0.277	-55.3	51.0	-0.30	0.148	-84.0	52.5	n/a	n/a	n/a	n/a	n/a	n/a	n/a	n/a	n/a	n/a	n/a			
		RIGHT	-0.15	0.426	-70.3	42.1	-0.23	0.269	-97.0	31.5	-0.34	0.062	-55.2	54.6	0.22	0.229	-68.9	27.4	-0.04	0.823	-25.6	106.0	-0.21	0.281	-64.1	59.7	0.01	0.975	-62.7	56.3	n/a	n/a	n/a	n/a	n/a	n/a	n/a	n/a	n/a	n/a	n/a			
SAD	INTENSE	LEFT	-0.36	0.050	-40.5	45.0	0.05	0.810	-93.9	26.8	-0.11	0.556	-51.8	34.5	-0.29	0.123	-30.5	48.3	0.17	0.375	-38.1	63.1	n/a	n/a	n/a	n/a	n/a	n/a	n/a	n/a	n/a	n/a	n/a	n/a	n/a	n/a	0.05	0.78	-52.9	46.2	0.04	0.85	-78.7	40.7
		RIGHT	-0.41	0.024	-100.7	-0.4	0.11	0.599	-16.2	85.7	-0.28	0.135	-91.4	9.9	-0.14	0.454	-50.9	41.6	0.04	0.839	-58.7	59.5	n/a	n/a	n/a	n/a	n/a	n/a	n/a	n/a	n/a	n/a	n/a	n/a	n/a	0.07	0.71	-50.1	66.2	-0.04	0.85	-65.9	44.0	
	MILD	LEFT	-0.37	0.045	-6.5	109.8	0.05	0.827	-70.9	46.8	-0.40	0.030	-40.2	77.4	0.03	0.862	-22.4	85.0	0.13	0.494	-80.6	57.4	n/a	n/a	n/a	n/a	n/a	n/a	n/a	n/a	n/a	n/a	n/a	n/a	0.01	0.94	-59.6	75.4	-0.21	0.32	-72.4	54.6		
		RIGHT	-0.24	0.206	-49.0	47.7	0.09	0.682	-20.0	83.9	-0.41	0.024	-62.6	35.1	0.23	0.230	-28.8	60.4	0.03	0.867	-28.7	85.2	n/a	n/a	n/a	n/a	n/a	n/a	n/a	n/a	n/a	n/a	n/a	-0.12	0.51	-50.1	62.1	0.03	0.88	-75.8	36.2			
	NEUTRAL	LEFT	-0.36	0.049	-70.1	21.7	-0.08	0.726	-12.4	133.1	-0.19	0.305	-43.5	49.3	-0.21	0.274	-68.1	16.6	-0.16	0.405	-20.5	87.6	n/a	n/a	n/a	n/a	n/a	n/a	n/a	n/a	n/a	n/a	n/a	0.06	0.74	-45.8	60.7	-0.03	0.87	-64.4	92.6			
		RIGHT	-0.34	0.068	-49.3	60.8	-0.08	0.702	-133.2	-17.2	-0.35	0.057	-61.1	50.2	-0.01	0.978	-42.8	58.8	0.08	0.675	-116.1	26.6	n/a	n/a	n/a	n/a	n/a	n/a	n/a	n/a	n/a	n/a	-0.08	0.67	-78.8	49.0	0.00	0.99	-52.7	72.3				

r = Pearson correlations between FC and demographic and clinical variables; CI, 95% confidence intervals; BD, bipolar disorder; HC, healthy controls; OFC, orbitofrontal cortex
HDRS-25 = Hamilton Depression Rating Scale-25 items; missing information about HDRS-25 in one rBD (25 year-old, male)
TASK PERFORMANCE in each emotion labeling task (sad and happy facial expression emotion labeling); missing information for three BD for the happy experiment
Statistical threshold of 0.05/12-p < 0.05, to control for multiple tests (2-tailed) in bold. Trend range 0.005-p < 0.05 in bold-italic.
All values reported are for BD. Just for 2 variables (AGE AT SCAN and HAPPY/SAD TASK PERFORMANCE), values are reported also in HC.

Table S4. Relationships between Dichotomous Clinical Variables and Amygdala-OFC Functional Connectivity in BD and HC

			Comorbidity* (OFF/ON)		Mood Stabilizers (OFF/ON)		Antipsychotics (OFF/ON)		Antidepressants (OFF/ON)		Benzodiazepines (OFF/ON)		Gender Effect in BD (MALE/FEMALE)		Gender Effect in HC (MALE/FEMALE)	
			T	P value	T	P value	T	P value	T	P value	T	P value	T	P value	T	P value
HAPPY	INTENSE	RIGHT	-0.65	0.523	0.09	0.929	-0.37	0.713	1.15	0.258	-0.23	0.820	-1.63	0.115	-0.49	0.627
		LEFT	-1.65	0.111	0.05	0.962	-0.38	0.704	-0.63	0.536	-2.29	0.030^a	1.47	0.152	1.59	0.137
	MILD	RIGHT	0.70	0.488	-0.58	0.568	0.18	0.861	1.50	0.145	-0.36	0.718	0.80	0.432	1.27	0.225
		LEFT	-0.19	0.849	-0.43	0.670	-0.51	0.615	0.90	0.374	-1.44	0.161	-0.63	0.541	-0.47	0.641
	NEUTRAL	RIGHT	-0.01	0.991	0.37	0.723	0.06	0.956	0.68	0.504	0.03	0.977	0.95	0.350	1.86	0.084
		LEFT	-0.22	0.824	0.18	0.857	-0.24	0.815	1.32	0.197	-0.82	0.419	0.43	0.667	1.23	0.238
SAD	INTENSE	RIGHT	0.25	0.802	0.76	0.454	-0.47	0.639	1.50	0.144	-0.31	0.764	0.72	0.482	0.81	0.426
		LEFT	-0.12	0.902	1.41	0.170	-1.13	0.268	1.37	0.183	-0.72	0.489	0.34	0.737	0.49	0.626
	MILD	RIGHT	0.65	0.525	0.71	0.487	0.02	0.983	1.51	0.142	-0.64	0.538	0.03	0.972	1.27	0.216
		LEFT	0.41	0.687	0.69	0.505	-0.16	0.873	3.99	0.001^b	-0.56	0.579	0.44	0.663	1.25	0.234
	NEUTRAL	RIGHT	-0.70	0.489	1.60	0.122	-0.83	0.416	0.52	0.609	-1.21	0.235	-0.97	0.342	-0.65	0.520
		LEFT	-1.14	0.264	0.50	0.621	0.19	0.848	0.05	0.957	0.42	0.679	-0.74	0.468	0.85	0.406

BD, bipolar disorder; HC, healthy controls; OFC, orbitofrontal cortex; FC, functional connectivity

* lifetime history of alcohol/substance abuse/dependence comorbidity; missing information about lifetime history of alcohol/substance abuse/dependence in four BD.

Statistics refer to between group differences (OFF/ON) in all BD and between gender difference (MALE/FEMALE) in BD and in HC. Statistical threshold of 0.05/12= $p \leq 0.005$, to control for multiple tests (2-tailed, in **bold**). Trend range 0.005< $p \leq 0.05$ in **bold-italic**.

^a BD taking benzodiazepines (mean[SD]=0.44[0.10]) had greater left amygdala-OFC FC to intense happy faces than BD not taking antidepressants (mean[SD]=0.36[0.10])

^b BD not taking antidepressants (mean[SD]=0.41[0.12]) had greater left amygdala-OFC FC to mild sad faces than BD taking antidepressants (mean[SD]=0.28[0.04]).

All values reported are for BD. Just for one variable (Gender Effect), values are reported in HC also.

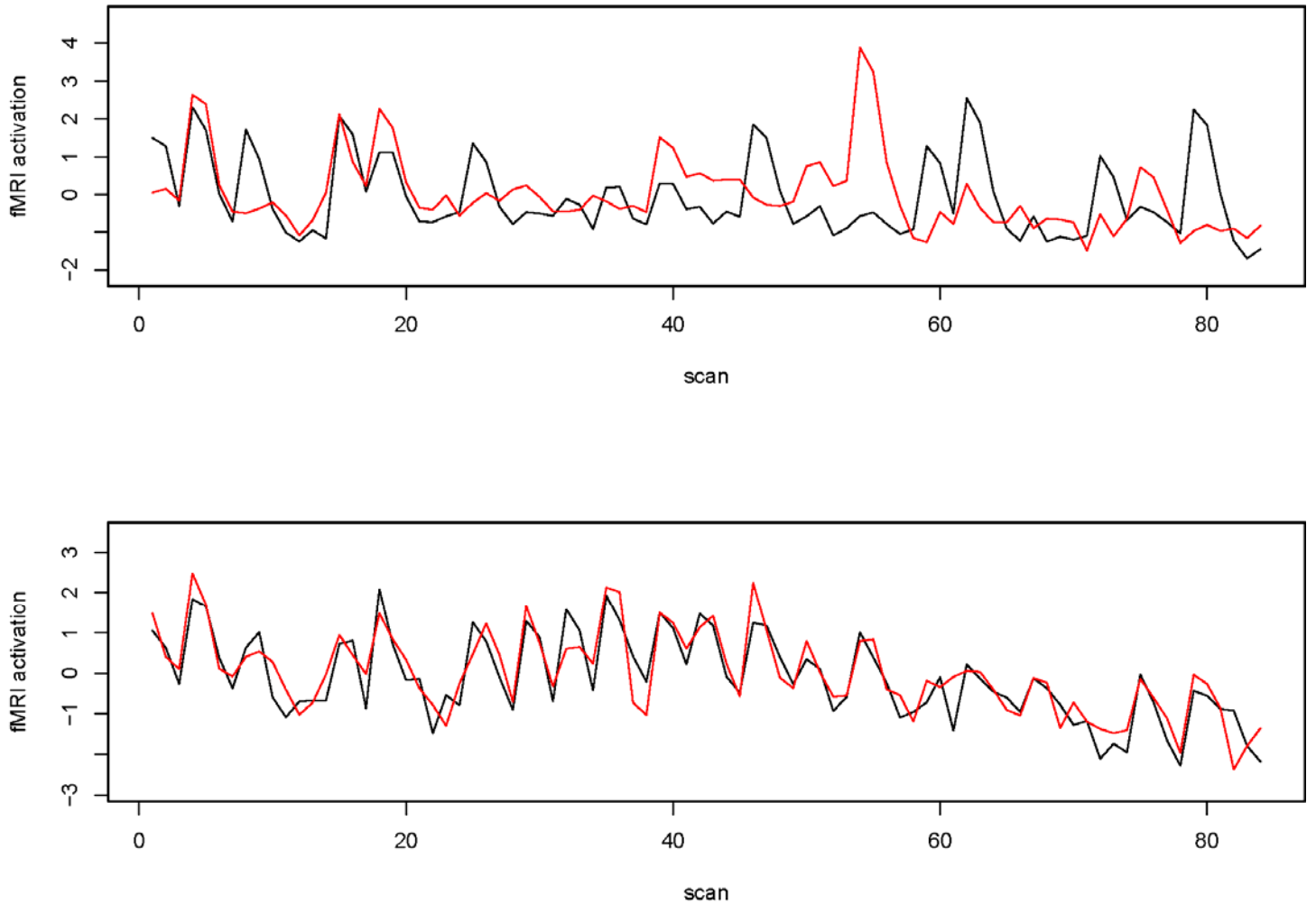


Figure S1. Mutual information is a measure of linear and non-linear dependence in two time series; it is zero if the two time series share no information (i.e., they are independent) and infinity if one time series is a deterministic function of the other. The mutual information of two time series can be computed in the frequency domain through the cross-coherence (10). Generally speaking, cross-coherence may be thought of as a correlation coefficient in the frequency domain. Mutual information is then computed by averaging the natural logarithm of one minus the coherence over all frequencies. A simple transformation is applied to the resulting measure to obtain a normalized mutual information (11) in the interval from zero to one, with zero indicating no shared information (independence) and 1 indicating perfectly shared information (complete dependence). Plots consist of simulated time series from pairs of regions

in an event-related design to demonstrate how mutual information measures dependence. The two regions in the top panel both activate to the stimulus but otherwise are weakly related. The cross-coherence at the stimulus frequency will be moderately high, but averaging over all frequencies will produce a modest measure of normalized mutual information of 0.24. The two time series in the bottom panel are more closely related both on and off trial frequencies. This results in considerably higher mutual information of 0.59. In our analyses we also accounted for stimulus effects upon time series by computing connectivity via partial mutual information by entering each stimulus-related response as a covariate. Here, we constructed a covariate waveform for each stimulus type (emotion intensity) in each experiment by convolving a canonical response with a delta function at the stimulus frequency.

Reference List

1. Phillips M, Ladouceur C, Drevets W (2008): A neural model of voluntary and automatic emotion regulation: implications for understanding the pathophysiology and neurodevelopment of bipolar disorder. *Mol Psychiatry*. 13:833-857.
2. Anjari M, Srinivasan L, Allsop JM, Hajnal JV, Rutherford MA, Edwards AD, et al. (2007): Diffusion tensor imaging with tract-based spatial statistics reveals local white matter abnormalities in preterm infants. *Neuroimage*. 35:1021-1027.
3. Karlsgodt KH, van Erp TG, Poldrack RA, Bearden CE, Nuechterlein KH, Cannon TD (2008): Diffusion tensor imaging of the superior longitudinal fasciculus and working memory in recent-onset schizophrenia. *Biol Psychiatry*. 63:512-518.
4. la-Maggiore V, Chan W, Peres-Neto PR, McIntosh AR (2002): An empirical comparison of SPM preprocessing parameters to the analysis of fMRI data. *Neuroimage*. 17:19-28.
5. Smith SM (2002): Fast robust automated brain extraction. *Hum Brain Mapp*. 17:143-155.
6. Smith SM, Jenkinson M, Woolrich MW, Beckmann CF, Behrens TEJ, Johansen-Berg H, et al. (2004): Advances in functional and structural MR image analysis and implementation as FSL. *Neuroimage*. 23:S208-S219.
7. Behrens TE, Woolrich MW, Jenkinson M, Johansen-Berg H, Nunes RG, Clare S, et al. (2003): Characterization and propagation of uncertainty in diffusion-weighted MR imaging. *Magn Reson Med*. 50:1077-1088.
8. Smith SM, Jenkinson M, Johansen-Berg H, Rueckert D, Nichols TE, Mackay CE, et al. (2006): Tract-based spatial statistics: Voxelwise analysis of multi-subject diffusion data. *Neuroimage*. 31:1487-1505.

9. Smith SM, Johansen-Berg H, Jenkinson M, Rueckert D, Nichols TE, Miller KL, et al. (2007): Acquisition and voxelwise analysis of multi-subject diffusion data with tract-based spatial statistics. *Nat Protoc.* 2:499-503.
10. Salvador R, Suckling J, Schwarzbauer C, Bullmore E (2005): Undirected graphs of frequency-dependent functional connectivity in whole brain networks. *Philosophical Transactions of the Royal Society B-Biological Sciences.* 360:937-946.
11. Granger CWJ, Lin JL (1995): Causality in the Long-Run. *Econometric Theory.* 11:530-536.